

# Radiative corrections to muon decays with massive Dirac neutrinos

P. Kalyniak

*TRIUMF and Physics Department, University of British Columbia,  
Vancouver, British Columbia, Canada V6T 2A6*

John N. Ng

*TRIUMF, 4004 Wesbrook Mall, Vancouver, British Columbia, Canada V6T 2A3*

(Received 5 October 1981)

We have calculated the first-order radiative corrections to the muon decay  $\mu^+ \rightarrow e^+ \nu_e \bar{\nu}_\mu$  along with the radiative decay  $\mu^+ \rightarrow e^+ \nu_e \bar{\nu}_\mu \gamma$  for the case of a single intermediate-mass Dirac neutrino mixing in the three-neutrino world. The method of dimensional regularization was used. The  $e^+$  spectra are shown for both unpolarized and polarized  $\mu^+$  decays.

Recently, there have been several experiments at the meson factories<sup>1,2</sup> to look for new structures in the weak interactions by precision measurements of the Michel parameters, in particular the  $\rho$  and  $\xi$  parameters, in the ordinary decay of muons,

$$\mu^+ \rightarrow e^+ \nu \nu' . \quad (1)$$

The radiative decay

$$\mu^+ \rightarrow e^+ \nu \nu' \gamma \quad (2)$$

has to be included in the consideration of Eq. (1) since the photon is not detected in these experiments.

The standard  $SU(2) \times U(1)$  gauge theory<sup>2</sup> with massless neutrinos differs from the prediction of the four-fermion  $V-A$  theory for the decay (1) by terms of order  $m_\mu^2/M_W^2$ . When radiative corrections are included the two theories differ<sup>3</sup> by terms of the order of  $\alpha m_\mu^2/M_W^2$ , where  $\alpha$  is the fine-structure constant. In fact, with radiative corrections the Michel parameter is modified to<sup>4,5</sup>

$$\rho^{\text{corr}} = 0.708 , \quad (3)$$

and this is to be compared with the uncorrected canonical value of  $\rho = 0.75$ . The experimental values<sup>6</sup> for  $\rho$  and  $\xi$  are

$$\rho^{\text{exp}} = 0.752 \pm 0.003 \quad (4a)$$

and

$$\xi^{\text{exp}} = 0.972 \pm 0.013 . \quad (4b)$$

The agreement between theory and experiment is

quite good.

Hence any deviation from the canonical values of  $\rho = \frac{3}{4}$  and  $\xi = 1$  in the new measurements would signal that new physics is operative. Otherwise, they will constrain the parameters of the possible new physics. One such new physics is the existence of right-handed  $W$  bosons coupling to the lepton families  $(\nu_\mu, \mu^-)_L$  and  $(\nu_e, e^-)_L$  at some detectable strength. Another source of possible deviations could be due to intermediate-mass neutrinos (IMN's), namely, neutrinos in the range of a few  $\text{MeV}/c^2$ , mixing into the light neutrinos. The second scheme does not require the existence of right-handed weak currents due to gauge bosons but could lead to other effects such as violation of  $\mu$ - $e$  universality in the branching ratio of pion decays and neutrino oscillations.<sup>7</sup>

In this paper we concentrate on the effects of IMN's on the precision measurements of  $\rho$  and  $\xi$ . In a previous paper hereafter referred to as I,<sup>8</sup> such effects on the free decay [reaction (1)] were discussed. We present the calculation including radiative corrections to reaction (1) and the radiative decay of reaction (2) for massive neutrinos.<sup>9</sup>

Next we give a brief discussion of the physics involved in the role an IMN plays in the precision measurements of  $\rho$  and  $\xi$ . As seen in I, the most interesting effect occurs at the high-energy end of the  $e^+$  spectrum, i.e., at  $x \equiv 2E_e/m_\mu$  near 1. In the standard  $V-A$  theory with massless neutrinos, angular momentum conservation calls for the  $e^+$  to come out with the maximum energy; in other words, the spectrum peaks at  $x = 1$  [see Fig. 1(a)].

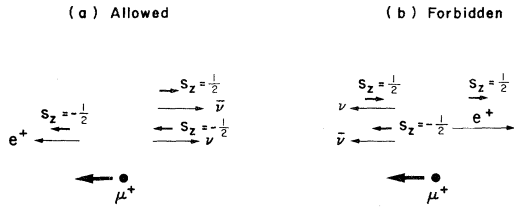


FIG. 1. Helicity considerations for the Michel spectrum for  $\mu^+$  decay with massless neutrinos. Angular momentum conservation allows the configuration (a) and forbids (b).

Similarly, if one examines the phase-space point of  $\vec{\sigma}_\mu \cdot \hat{p}_e = -1$ , where  $\sigma_\mu$  is the spin of the  $\mu^+$ , the spectrum should vanish if chirality is good. These are precisely the predictions of the  $V-A$  theory with massless neutrino. Hence, any mechanism that violated chirality conservation would lead to a decrease from maximum of the spectrum at  $x \simeq 1$  and also a nonvanishing spectrum at  $\vec{\sigma}_\mu \cdot \hat{p}_e = -1$ . Two such possibilities are right-handed currents or massive neutrinos with predominantly left-handed interactions. For the latter, the amount of the deviation from the standard values will be controlled by  $(m_\nu/m_\mu)^2$  and the mixing angle between the heavy and the two light neutrinos. In this paper we always assume that the neutrinos in the doublets  $(\nu_\mu, \mu^-)_L$  and  $(\nu_e, e^-)_L$  are predominantly light neutrinos.<sup>10</sup>

It was observed a long time ago<sup>5</sup> that radiative corrections would change significantly the Michel spectrum. For the decay of unpolarized muons, the tip of the spectrum at  $x=1$  is brought down from its maximum to the value zero when virtual radiative corrections to reaction (1) and the bremsstrahlung process of reaction (2) are included. Since radiative correction is large at the edge of the phase space for the standard theory with massless neutrinos, it is not *a priori* clear that such corrections to the massless case would be small. As we shall see later, the corrections are also large just as in the massless-neutrino case. It is the purpose of this paper to establish quantitatively the effects of radiative corrections to massive Dirac neutrinos. Since we have shown in I that the difference<sup>11</sup> between Dirac and Majorana neutrinos is very small for the Michel spectrum, we expect this is true when radiative corrections are included. Hence, for simplicity we work only with Dirac neutrinos.

Our next simplifying assumption involves the mixing of the neutrinos. Within the framework of  $SU(2) \times U(1)$  gauge theory with  $N$  lepton doublets,

the neutrino weak eigenstates  $\nu_a$  are related by an  $N \times N$  unitary transformation to the mass eigenstates  $\nu_i$ . Explicitly,

$$|\nu_a\rangle = \sum U_{ai} |\nu_i\rangle, \quad (5)$$

where  $a = e, \mu, \tau, \dots$  and  $i = 1, 2, 3, \dots$ . We also order the masses of the neutrinos  $m_i$  such that  $m_1 < m_2 < \dots < m_N$ . Furthermore, we assume that the mixing is hierarchical, i.e.,  $U_{e1} > U_{e2} > U_{e3}$ , etc. and the dominant matrix elements lie in the diagonal. The next dominant elements are the ones immediately next to the diagonal. We shall call this case the hierarchical-nearest-neighbour (HNN) mixing scheme. This is expected from grand unified models. From a naive extrapolation of our knowledge of the mixings of charge  $-\frac{1}{3}$  quarks we expect the  $\nu$  mixings to be as indicated above. Thus we only need to keep terms that involve at most one heavy neutrino in the decay of the muon. Recent experiments<sup>10</sup> give  $10 < m_1 < 40$  eV/ $c^2$  and  $m_2 < 0.5$  MeV/ $c^2$ . This holds if one assumes that  $\nu_e$  is principally  $\nu_1$  and  $\nu_\mu$  is mainly  $\nu_2$ . Within the accuracy of the muon decay experiments we can set  $m_1 \approx m_2 \simeq 0$ . However,  $\nu_3$  can be heavy<sup>12</sup> and can have a detectable mixing with  $\nu_1$  and/or  $\nu_2$ . In our numerical calculations we will deal only with the case of a three-neutrino world with  $\nu_3$  or  $\nu_\tau$  heavy in the MeV/ $c^2$  range. Presently, the general  $N$ -neutrino world will involve so many unknown parameters as to render a numerical analysis meaningless.

It was shown<sup>3</sup> that the difference between the  $SU(2) \times U(1)$  theory and the four-Fermion theory is very small at low energies; hence, we shall use the four-fermion theory to calculate the photonic radiative corrections. Doing it in the full-fledged  $SU(2) \times U(1)$  gauge theory will only give corrections to the order of  $\alpha(m_\mu^2/M_W^2)$  to our results. As in the massless neutrinos case both the ultraviolet and infrared divergences cancel to order  $\alpha$  and a finite answer emerges.<sup>5,9</sup> In fact, the terms involving neutrino mass can be factored out cleanly. We shall use the technique of dimensional regularization<sup>13</sup> to regulate the divergent integrals that occur. To our knowledge this is the first time a complete calculation of muon decay using this technique is presented. The infrared part of the problem for massless neutrinos was discussed in Ref. 14 using the dimensional regularization technique. Next we will present the results of our calculations. The theoretical details of dimensional regularization and the cancellation of divergences are given in the Appendix.

The  $e^+$  spectrum for the decay of  $\mu^+$  at rest is given by

$$2E_e \frac{d^3R}{d^3p_e} = 2E_e \sum_{i,j}^{N'} |U_{\mu i}|^2 |U_{ej}|^2 \frac{d^3R_{ij}}{d^3p_e}, \quad (6)$$

where  $N'$  is the number of neutrinos that can

kinematically couple to the processes (1) and (2). Within the framework of  $SU(2) \times U(1)$  theory of dominant left-handed weak interactions only,  $N' \leq N$ , the total number of lepton doublets. Under our assumption of hierarchal mixing only neutrinos in the same doublet of  $\mu$  and  $e$  or the nearest-neighboring doublet contribute to the sum. Thus, after performing the azimuthal angular<sup>15</sup> (see I) integration

$$\frac{d^2R}{d \cos \theta dx} \simeq \frac{G_F^2 m_\mu^5}{192\pi^3} [ (|U_{\mu 1}|^2 + |U_{\mu 2}|^2)(|U_{e 1}|^2 + |U_{e 2}|^2)R_0 + |U_{\mu 3}|^2(|U_{e 1}|^2 + |U_{e 2}|^2)R_3 ], \quad (7)$$

where we have used  $m_{1,2} \simeq 0$  and  $x \equiv 2E_e/m_\mu$ , and the angle the emitted  $e^+$  makes with the  $z$  axis is denoted by  $\theta$ . The quantity  $R_0$  is the usual radiatively corrected spectrum for massless neutrinos and  $R_3$  is the spectrum when only one massive neutrino enters the decay. Hence, the correction to the Michel spectrum is due to  $R_3$  and is proportional to the strength of the mixing  $|U_{\mu 3}|^2$ . In the three-neutrino world, unitarity of  $U$  gives  $|U_{e 1}|^2 + |U_{e 2}|^2 = 1 - |U_{e 3}|^2$ . Under the nearest-neighbor hierarchal mixing assumption this factor is approximately unity. However, the kinematic factor in  $R_3$  enhances this effect. The result for  $R_0$  is well known and is given by<sup>9</sup>

$$R_0 = R_0^f + R_0^c, \quad (8a)$$

$$R_0^f = x^2(3-2x) - \vec{\sigma}_\mu \cdot \hat{p}_e x^2(1-2x), \quad (8b)$$

$$R_0^c = \frac{\alpha}{\pi} \left\{ x^2(3-2x)r(x) - \frac{3}{2}x^2 \ln x + \frac{1-x}{6} \left[ (5+17x-34x^2) \left( \ln \frac{x}{\delta_e} \right) - 22x + 34x^2 \right] - \vec{\sigma}_\mu \cdot \hat{p}_e R_{os}^c \right\}, \quad (8c)$$

and the spin-dependent term is

$$R_{os}^c = \frac{\alpha}{\pi} \left\{ x^2(1-2x)r(x) - \frac{x^2}{2} \ln x - \frac{(1-x)}{6} \left[ (1+x+34x^2) \ln \left( \frac{x}{\delta_e} \right) + 3-7x-32x^2 + \frac{4}{x}(1-x)^2 \ln(1-x) \right] \right\}, \quad (8d)$$

where

$$r(x) = \left( \ln \frac{x}{\delta_e} - 1 \right) \left[ 2 \ln \frac{1-x}{x} + \frac{3}{2} \right] + \ln(1-x) \left[ \ln x - \frac{1}{x} + 1 \right] - \ln x + 2\text{Li}_2(x) - \frac{\pi^2}{3} - \frac{1}{2} \quad (8e)$$

with  $\delta_e \equiv m_e/m_\mu$  and  $\vec{\sigma}_\mu$  is the spin of the  $\mu^+$  and  $\hat{p}_e$  the unit vector of the outgoing  $e^+$ . The dilogarithm or Spence's function  $\text{Li}_2(x)$  is defined by

$$\text{Li}_2(x) = - \int_0^x dt \frac{\ln(1-t)}{t} \quad (t \leq 1). \quad (9)$$

The massive neutrino spectrum  $R_3$  is calculated in the Appendix. We divide it into a free-decay piece  $R_3^f$  and the radiatively corrected piece

$$R_3 = R_3^f + R_3^c. \quad (10a)$$

The first piece  $R_3^f$  was calculated in I and is given by

$$R_3^f = \frac{x^2(1-x-\delta^2)}{(1-x)^3} \left\{ 2[(1-x)^2 + \delta^2(1-x) - 2\delta^4] + \left[ 1 - \frac{x}{2} + \frac{x}{2} \vec{\sigma}_\mu \cdot \hat{p}_e \right] \right. \\ \left. + (1-x)[(1-x)^2 - 2(1-x)\delta^2 + \delta^4](1 - \vec{\sigma}_\mu \cdot \vec{p}_e) \right\} \theta(1-\delta^2). \quad (10b)$$

The radiative correction to it is explicitly presented as

$$R_3^c = R_0^c + \frac{\alpha x}{\pi} \left\{ x[-3\bar{\delta}^2(1-x) - 3\bar{\delta}^4 + \bar{\delta}^6(3-x)]r(x) \right. \\ + \bar{\delta}^2 \left[ \frac{21}{2} - \frac{27}{2}x + \frac{17}{2}x^2 - \frac{3}{2} \frac{x^2 \ln x}{(1-x)} + \frac{1}{2x}(-9-3x+21x^2-17x^3) \ln(x/\delta_e) \right] \\ + \bar{\delta}^4 \left[ -9-3x-x^2 + \frac{3x(1-3x)}{2(1-x)} \ln x + \frac{1}{2x}(9+9x^2+2x^3) \ln(x/\delta_e) \right] \\ + \bar{\delta}^6 \left[ \frac{1}{6}(13+43x-11x^2) + \frac{x(-3+8x)}{2(1-x)} \ln x + \frac{1}{6x}(-5-3x-39x^2+11x^3) \ln \frac{x}{\delta_e} \right] \\ + [\ln(1-\bar{\delta}^2)](1-\ln x/\delta_e)[-2x(3-2x) + 6\bar{\delta}^2x(1-x) + 6\bar{\delta}^4x + 2\bar{\delta}^6x(-3+x)] \\ - 3\bar{\delta}^4 \ln \bar{\delta}^2 \left[ 2x + \frac{1}{x}(1-2x-x^2) \ln x/\delta_e \right] \\ \left. + \bar{\delta}^6 \ln \bar{\delta}^2 \left[ 1+4x-x^2 + \frac{1}{x}(1-3x-3x^2+x^3) \ln x/\delta_e \right] \right\} \theta(1-\delta^2) - \vec{\sigma}_\mu \cdot \hat{p}_e R_{3s}^c, \quad (10c)$$

and

$$R_{3s}^c = R_{0s}^c + \frac{\alpha x}{\pi} \left\{ x[-3\bar{\delta}^2(1-x) + 3\bar{\delta}^4 - \bar{\delta}^6(1+x)]r(x) \right. \\ + \bar{\delta}^2 \left[ \frac{1}{2x}(3-12x-8x^2+6x^3) - \frac{3}{x^2}(1-x)^3 \ln(1-x) + \frac{(12-48x+75x^2-39x^3+9x^4)}{2x^2(1-x)} \ln x \right. \\ \left. + \frac{1}{2x}(3-3x+17x^2-3x^3) \ln x/\delta_e \right] \\ + \bar{\delta}^4 \left[ \frac{1}{2x}(-15+42x-13x^2+12x^3) - \frac{3x(1-3x)}{2(1-x)} \ln x + \frac{1}{2x}(3-12x-5x^2-6x^3) \ln x/\delta_e \right] \\ + \bar{\delta}^6 \left[ \frac{1}{6x}(39-100x+56x^2-46x^3) + \frac{x(1-4x)}{2(1-x)} \ln x + \frac{11(1-x)^3}{6x^2} \ln(1-x) \right. \\ \left. + \frac{1}{6x}(-17+45x-27x^2+35x^3) \ln x/\delta_e \right] \\ + \bar{\delta}^4 \ln \bar{\delta}^2 \left[ \frac{3}{x}(-1+2x-x^2) + \frac{3(1-2x-x^2)}{x} \ln x/\delta_e - \frac{12(1-x)^3}{x^2} \ln(1-x) \right] \\ \left. + \bar{\delta}^6 \ln \bar{\delta}^2 \left[ \frac{1}{x}(-3+8x-9x^2) + \frac{1}{x}(1-3x+5x^2+x^3) \ln \frac{x}{\delta_e} - \frac{2(1-x)^3}{x^2} \ln(1-x) \right] \right\} \theta(1-\delta^2), \quad (10d)$$

TABLE I. Corrections to the polarization  $P$  of the  $\mu^+$  from  $\pi^+ \rightarrow \mu^+ \nu$  decay due to the mixing of massive neutrinos [see Eqs. (12) and (13)].

$m_2$ (MeV/c <sup>2</sup> )	$P_\nu$	$P( U_{23} ^2=0.0588)$	$P( U_{23} ^2=0.067)$	$P( U_{23} ^2=0.1)$
0	1	1	1	1
3	0.9912	0.9995	0.9994	0.9991
5	0.9757	0.9986	0.9984	0.9976
10	0.9055	0.9944	0.9937	0.9906

where  $r(x)$  is given by Eq. (8e). In the above equations terms that are multiplied by  $\delta_e^2$  and higher in powers of  $\delta_e$  are dropped but we retain  $\ln\delta_e$  terms; also  $\bar{\delta}^2 \equiv \delta^2/(1-x)$ . Owing to the presence of  $\bar{\delta}^2$  terms and not only  $\delta^2$ , the effects of radiative corrections for massive neutrinos are very important near the upper end of the spectrum, namely,  $x$  close to  $1-\delta^2$ .

Both the terms  $R_0$  and  $R_3$  have a singularity as  $x \rightarrow 1$  coming from  $\ln(1-x)$ . This is due to the famous infrared catastrophe of a charged particle's capability of emitting a large number of soft photons. We have adopted Källén's smearing procedure for the term  $\ln(1-x)$  by making the replacement<sup>9</sup>

$$\ln(1-x) \rightarrow \ln(1-x + \Delta x) \quad (11)$$

for  $x$  near 1 and  $(m_\mu/2)\Delta x =$  energy resolution of the apparatus. An alternative procedure of exponentiating these terms has also been suggested.<sup>10</sup> The practical differences of these two procedures are small. Furthermore, Eqs. (8) and (10) are also not applicable for  $x$  very close to the origin due to our omission of  $\delta_e$  terms as well as the importance of the two-photon contributions. For the measurements of  $\rho$  and  $\xi$  the formulas [see Eqs. (8)–(10)] are sufficiently accurate.

We also observe that no additional mass singularities due to  $m_\nu \neq 0$  are present in  $R_3$ ; i.e., no terms of the type  $\ln\delta$  appear. All logarithmic terms of  $\delta$  are correctly accompanied by powers of  $\delta^2$  and thus vanish in the limit  $\delta \rightarrow 0$ . Hence, the only mass singularities are due to the electron mass, i.e.,  $\ln\delta_e$  terms. This is precisely as expected from the Lee-Nauenberg-Kinoshita<sup>16,17</sup> theorem.

The spin terms involving  $\vec{\sigma}_\mu \cdot \hat{p}_e \equiv P \cos\theta_e$  are relevant for the measurement of the  $\xi$  parameter, where  $P$  is the polarization of the  $\mu^+$ . We have defined the angle  $\theta_e$  to be that between the direction of the outgoing  $e^+$  and the initial polarization  $P$  of the  $\mu^+$ . However, due to the presence of the intermediate-mass neutrino the initial polarization  $P$  of the  $\mu^+$  from  $\pi^+ \rightarrow \mu^+ \nu$  decay is not 1 but is

given by

$$P = 1 - |U_{\mu 3}|^2 + |U_{\mu 3}|^2 P_\nu \quad (12)$$

and

$$P_\nu = \frac{(1-\delta^2)\lambda^{1/2} \left[ 1, \frac{m_\mu^2}{m_\pi^2}, \frac{m_\nu^2}{m_\pi^2} \right]}{(1+\delta^2) \left[ 1 - \frac{m_\mu^2}{m_\pi^2} - \frac{m_\nu^2}{m_\pi^2} \right] + 4 \frac{m_\nu^2}{m_\pi^2}}, \quad (13)$$

where  $\lambda(x, y, z) = x^2 + y^2 + z^2 - 2xy - 2yz - 2zx$ , and we have assumed only the third neutrino with mass

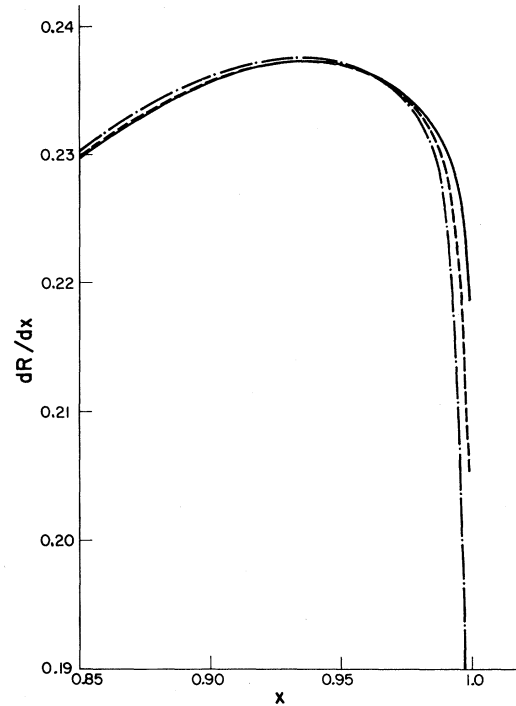


FIG. 2. The tip of the Michel spectrum for a 5-MeV/c<sup>2</sup> neutrino with mixing  $|U_{\mu 3}|^2 = 0.059$  (dashed curve) and  $|U_{\mu 3}|^2 = |U_{e 3}|^2 = 0.1$  (dash-dot curve). The solid curve is the standard Michel spectrum. The curves are normalized with respect to each other.

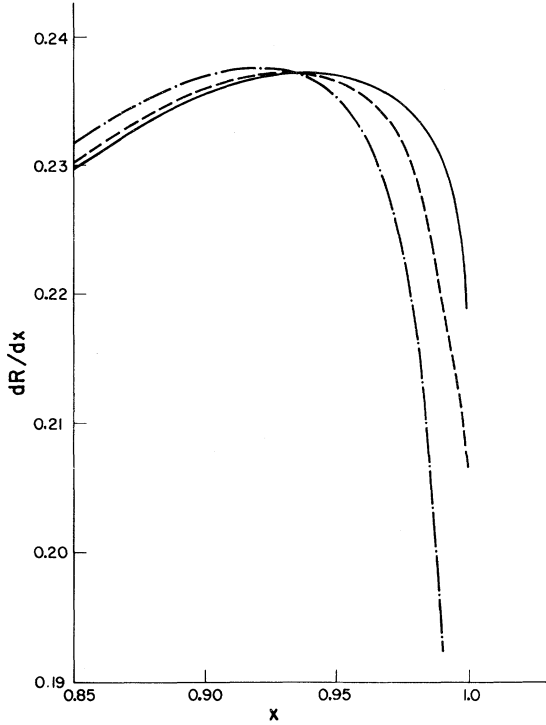


FIG. 3. High-energy end of the Michel spectrum for a 10-MeV/ $c^2$  neutrino with  $|U_{\mu 3}|^2 = 0.059$  (dashed curve) and equal mixing of  $|U_{\mu 3}|^2 = |U_{e 3}|^2 = 0.1$  (dash-dot curve). The solid curve is the standard Michel spectrum. The curves are normalized with respect to each other.

$m_\nu$  is significantly coupled to  $\mu^+$ . The decrease of  $P$  from the value of unity for different values of  $\delta$  and mixing parameter is given in Table I. It is seen that the polarization is not very different from unity for most cases unless both the mass  $m_\nu$  and the mixing  $|U_{\mu 3}|$  are large. Recent experiments<sup>17</sup> of the  $\mu^+$  spectrum for  $\pi_{l2}$  decays have ruled out a large mixing for neutrinos of mass  $m_\nu > 10$  MeV/ $c^2$ . However, no information is given for  $m_\nu < 10$  MeV/ $c^2$  due to the energy resolution.<sup>18</sup>

In Fig. 2 we plot the radiatively corrected Michel spectrum for a 5-MeV/ $c^2$  neutrino for different values of  $U_{\mu 3}$ . Note that the shape of the spectrum for massive neutrinos when radiatively corrected looks very similar to the massless spectrum even at the edge where  $x \simeq 1$ . The standard  $m_\nu = 0$  case is also given as a reference. We start out at  $x = 0.85$  since  $\delta \neq 0$  gives no visible alteration to the spectrum for  $x < 0.85$ . The curves are normalized relative to each other for a given mass and mixing.

Figure 3 shows the high-energy end of the

Michel spectrum for a 10-MeV/ $c^2$  neutrino. It is seen that distinguishing between massive neutrinos and the massless neutrino spectrum is very difficult if the mixing  $|U_{\mu 3}|^2$  is small. For  $m_\nu = 10$  MeV/ $c^2$  a mixing  $\lesssim 0.02$  is possible. In general there are two features to look for. There is a kink at  $x = 1 = \delta^2$  which is  $x = 0.990$  for  $m_\nu = 10$  MeV/ $c^2$  and  $x = 0.9998$  for  $m_\nu = 5$  MeV/ $c^2$ . The latter is currently unmeasurable. The maximum of the Michel spectrum also shifts towards lower values of  $x$  compared to the massless case. Either of these two effects are difficult to measure.

In Fig. 4 we give the values of  $U_{\mu 3}$  that are allowed by the current data<sup>19</sup> of the  $\rho$  measurement as a function of the neutrino mass  $m_\nu$ . Under the HNN assumption for 10 MeV/ $c^2$  only a very small mixing  $|U_{\mu 3}|^2 \lesssim 0.025$  is allowed. Similarly for  $m_\nu = 3$  MeV/ $c^2$  we have  $|U_{\mu 3}|^2 \lesssim 0.185$  although this mass is beyond the energy range of  $\pi_{l2}$  due to the energy resolutions of current experiments. In

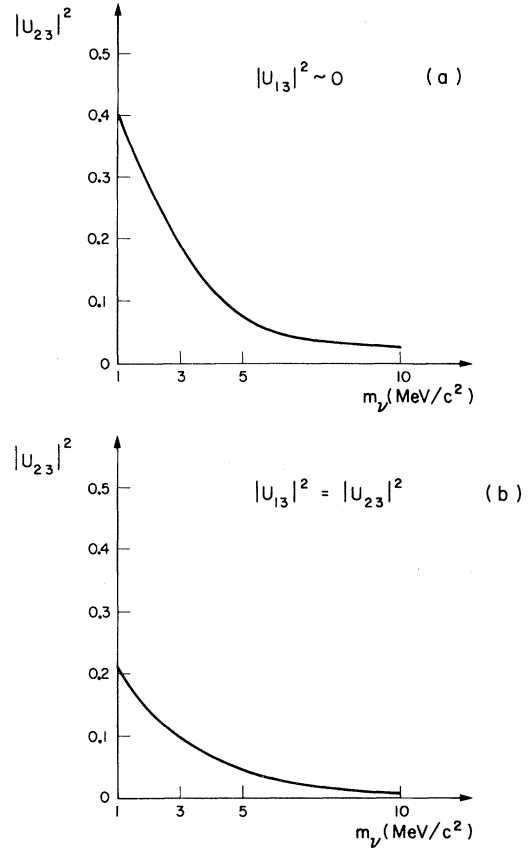


FIG. 4. Limits of allowed mixing of  $|U_{\mu 3}|^2$  as a function of neutrino mass. Hierarchical-nearest-neighbor mixing is depicted in (a), and (b) gives the case for equal mixing.

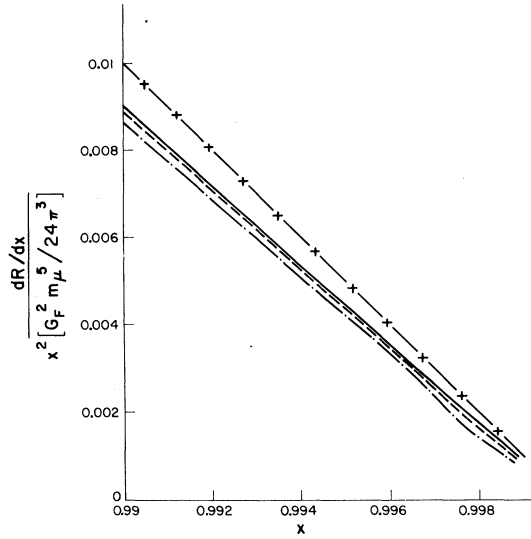


FIG. 5. High-energy end of Michel spectrum with spin of  $\mu^+$  antiparallel to the direction of emitted  $e^+$ . For  $m_\nu = 5 \text{ MeV}/c^2$ , the dash-dot curve stands for  $|U_{\mu 3}|^2 = |U_{e 3}|^2 = 0.1$  and the dashed curve for  $|U_{\mu 3}|^2 = 0.067$ . The massless neutrino with radiative corrections case is depicted by the solid line. For reference the dash-cross line is the case with no radiative corrections and is of the form  $y = 1 - x$ . The curves are arbitrarily normalized and displaced from each other to reveal the difference.

Fig. 4(b) we plot the same for equal mixing in a three-neutrino world.

Next we discuss the spin terms. Looking at Fig. 1 we conclude that angular momentum forbids the  $e^+$  in the forward direction if the initial polarization of the  $\mu^+$  is pointing in the  $-\hat{z}$  direction. This is reflected in Eq. (8b) where  $R_0 = 0$  at  $x = 1$  for  $\vec{\sigma}_\mu \cdot \hat{p}_e = -1$ . Equation (8b) is for massless neutrinos where chirality is good. This feature is again preserved when radiative corrections are taken into account as can be seen by setting  $\vec{\sigma}_\mu \cdot \hat{p}_e = -1$  in Eq. (8c) and evaluating it at  $x = 1$ . With the mixing of a massive neutrino the spectrum for  $\vec{\sigma}_\mu \cdot \hat{p}_e = -1$  does not vanish at  $x = 1$  in a linear fashion. Figure 5 depicts the correction for  $m_\nu = 5$

$\text{MeV}/c^2$  and  $|U_{\mu 3}|^2 = 0.067$ , i.e., Cabibbo-type mixing and also for  $|U_{\mu 3}|^2 = |U_{e 3}|^2 = 0.1$ . Again only for the latter case can one discern a deviation from the massless-neutrino situation.

## CONCLUSION

We have calculated the first-order radiative correction to the decay of a  $\mu^+$  at rest plus the bremsstrahlung decay with one massive neutrino mixing into the  $(e, \nu_1)_L$  and  $(\mu, \nu_2)_L$  doublets. Both the  $e^+$  spectrum [Eqs. (7)–(10d)] and the bremsstrahlung spectra [Eq. (A21)] are given. The assumptions we made are that weak interactions are predominantly left-handed and that significant mixing only occurs between the nearest-neighbor families of lepton doublets in the standard picture. Our result can be generalized to include any intermediate-mass neutrino that may have a large mixing with  $\nu_\mu$  and  $\nu_e$ . Obviously, by changing the parameters  $\delta_1$  and  $\delta_2$  and  $m_\mu$  we can use the results for  $\tau^+$  decays or any three-body leptonic decays of heavy leptons.

We found that for IMN's with small mixing the deviations from the standard massless-neutrino spectra are small. In previous calculations where no radiative corrections are included sensitivity of the Michel spectrum at  $x$  near 1 to IMN's was found.<sup>8</sup> Here we report that this sensitivity is mostly reduced when first-order radiative correction is included in the calculation, so that the spectra look qualitatively the same. Quantitative difference, however, still remains but is very difficult to detect experimentally.

The asymmetry measurement is also largely unaffected by IMN's if their mixing is of the order of Cabibbo mixing or less (see Fig. 5). An IMN with large mixing is unlikely since it gives rise to additional peaks in  $\pi_{l2}$  decays as well as including a large deviation from the universality in the  $\pi_{e\nu}/\pi_{\mu 2}$  branching ratio.

Alternatively, our results can be interpreted as the  $\nu_\tau$  must have a mass less than  $5 \text{ MeV}/c^2$  if it

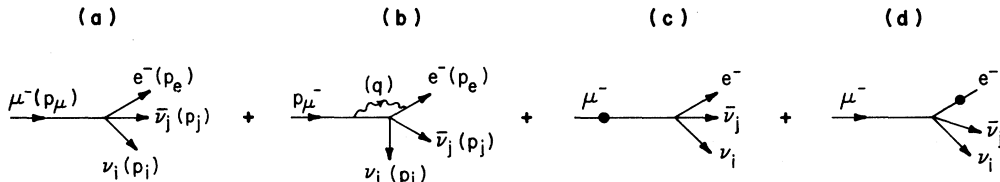


FIG. 6. Feynman diagrams for the free-muon decay plus the virtual-photon corrections. The black dots in (c) and (d) are the self-energy corrections.

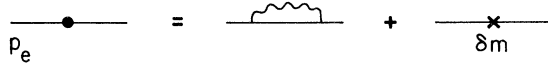


FIG. 7. Self-energy correction diagrams of the charged leptons.

mixes with  $\nu_\mu$  with a strength of the order of Cabibbo mixing.

#### ACKNOWLEDGMENTS

We would like to thank Dr. C. Oram for discussion on the TRIUMF experiment on the measurement of the  $\xi$  parameter. Conversations with Professor D. Beder were very helpful. One of the authors (J.N.N.) would like to thank Professor L. S. Brown and Professor S. Ellis for the kind hospitality at the University of Washington Theoretical Physics Summer Institute where this work was completed.

#### APPENDIX

The relevant Feynman diagrams are depicted in Figs. 6 and 7. The interference between graph Fig. 6(a) and the sum of Figs. 6(b)–6(d) gives the radiative correction to the reaction (1). The bremsstrahlung graphs of Figs. 8(a) and 8(b) are calculated separately and the double-differential cross section is given. This will be of use for some future experiments that measure the photon spectrum. To obtain the correction to the Michel spectrum due to the bremsstrahlung process, we integrate over the undetected photon. It is well known that the diagram Figs. 6(b)–6(d) and Fig. 7 have ultraviolet and infrared divergences. We use the dimensional regularization procedure of 't Hooft and Veltman<sup>13</sup> to deal with both problems at once. To our knowledge this is the first time a complete calculation to the  $\mu$ -decay process using this technique is presented.

The convention for the Dirac  $\gamma$  matrices in  $n$  dimensions is as follows:<sup>20</sup>

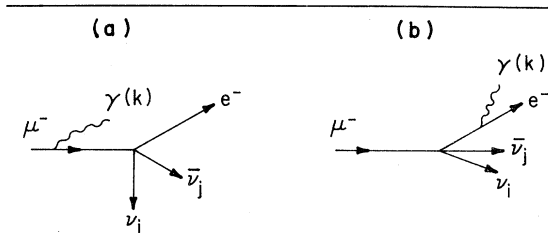


FIG. 8. Bremsstrahlung graphs correction to free-muon decays.

$$\{\gamma_\mu, \gamma_\nu\} = 2g_{\mu\nu}, \quad (\text{A1})$$

$$\gamma^\mu \gamma_\mu = n, \quad (\text{A2})$$

$$\text{Tr} 1 = n, \quad (\text{A3})$$

$$\text{Tr} \gamma^\mu \gamma^\nu \gamma^\rho \gamma^\omega = n(g^{\mu\nu} g^{\rho\omega} - g^{\mu\rho} g^{\nu\omega} + g^{\mu\omega} g^{\nu\rho}), \quad (\text{A4})$$

$$\text{Tr} \gamma^{\mu_1} \dots \gamma^{\mu_m} = 0, \text{ for } m = \text{odd}, \quad (\text{A5})$$

and

$$\gamma_\mu \gamma_\alpha \gamma^\mu = (2-n)\gamma_\alpha. \quad (\text{A6})$$

The prescription for  $\gamma_5$  we used is that of Ref. 13, i.e.,

$$\{\gamma_5, \gamma_\mu\} = 0, \quad \mu = 0, 1, 2, 3 \quad (\text{A7})$$

and

$$[\gamma_5, \gamma_\mu] = 0, \quad \mu = 4, \dots, n-1. \quad (\text{A8})$$

The external lepton lines in Fig. 6 are taken to be four-dimensional vectors and are not continued to  $n$  dimensions.

In  $n$  dimensions the coupling  $e_0$  is scaled by a dimensional parameter. We shall choose the natural scale of the muon mass; thus,

$$e_0 = (m_\mu^2)^{2-n/2} e, \quad (\text{A9})$$

where  $e$  is a dimensionless quantity in  $n$  dimensions.

In the Feynman gauge the sum of the two self-energy graphs of Fig. 7 gives, after subtraction of the appropriate mass counterterm,

$$S^\lambda = \frac{-e^2}{8\pi^2} \left[ 3 \left[ \frac{2}{4-n} - \gamma_E - \ln \delta_e \right. \right. \\ \left. \left. + 2 \ln 2\sqrt{\pi} \right] + 4 \right] \bar{e} \gamma^\lambda \frac{(1-\gamma_5)}{2} \mu, \quad (\text{A10})$$

where  $\gamma_E$  is the Euler-Mascheroni constant.

Similarly after some manipulation of the Dirac algebra and integrating over the virtual-photon momentum in  $n$  dimensions, we obtain the vertex correction (see Fig. 6) to be

$$\begin{aligned}
V^\lambda = \frac{e^2}{8\pi^2} \left\{ \left[ 2 \left[ \frac{1}{4-n} + \ln 2\sqrt{\pi} - \frac{\gamma_E}{2} \right] \left[ \ln \frac{x^2}{\delta_e^2} + 1 \right] \right. \right. \\
+ 2 \left[ \ln^2 \delta_e + \ln x \ln \frac{1-x}{x} - \frac{\pi^2}{6} + \text{Li}_2(x) \right] - 4 \ln \delta_e + \ln x \left[ 3 - \frac{1}{1-x} \right] \left. \right] \bar{e} \gamma^\lambda \frac{(1-\gamma_5)}{2} \mu \\
- \frac{1}{1-x} \left[ \frac{p_e^\lambda}{m_\mu} \left[ 1 + \frac{2x-1}{1-x} \ln x \right] - \frac{p_\mu^\lambda}{m_\mu} \left[ 1 + \frac{x}{1-x} \ln x \right] \right] \left. \right] \bar{e} \frac{1+\gamma_5}{2} \mu \left. \right\}, \quad (\text{A11})
\end{aligned}$$

where we have neglected all terms  $O(\delta_e^2)$ . The ultraviolet divergence of the graph appears as a pole in  $n=4$ . The photonic virtual corrections to the electron spectrum are then given by multiplying with the amplitude of the free-decay graph (see Figs. 6 and 7) and integrating over the phase space of the two outgoing neutrinos. Thus, with only the  $i$ th neutrino being of intermediate mass,

$$\begin{aligned}
\left[ \frac{dR_{ij}}{dz dx} \right]_{\text{virtual}} &= \frac{\alpha}{2\pi} \frac{G_F^2 m_\mu^5 x}{192\pi^3} |U_{\mu i}|^2 |U_{ej}|^2 \\
&\times \left\{ \frac{x(1-\bar{\delta}_i^2)^2}{1-x} \left[ (1+2\bar{\delta}_i^2)(2-2x+3x \ln x) \right. \right. \\
&\quad - (2+\bar{\delta}_i^2)(1-x) \left[ 1 + \frac{x}{1-x} \ln x \right] \left. \right] (1-\vec{\sigma}_\mu \cdot \hat{p}_e) \\
&\quad + 2x(1-\bar{\delta}_i^2)^2 \{ (1+2\bar{\delta}_i^2)(2-x) + (1-x)(1-\bar{\delta}_i^2) \\
&\quad \left. \left. + \vec{\sigma}_\mu \cdot \hat{p}_e [(1-\bar{\delta}_i^2)(1-x) - (1+2\bar{\delta}_i^2)x] \} F \right\}, \quad (\text{A12})
\end{aligned}$$

where

$$\begin{aligned}
F = \left[ \frac{1}{4-n} - \frac{\gamma_E}{2} + \ln 2\sqrt{\pi} \right] \left[ \ln \frac{x^2}{\delta_e^2} - 2 \right] - \frac{\pi^2}{6} + \text{Li}_2(x) + \ln^2 \delta_e \\
+ \ln x \ln(1-x) - \ln^2 x - \frac{1}{2} \ln \delta_e + \frac{1}{2} \left[ 3 - \frac{1}{1-x} \right] \ln x - 2 \quad (\text{A13})
\end{aligned}$$

and

$$\bar{\delta}_i^2 = \frac{\delta_i^2}{1-x}. \quad (\text{A14})$$

In the limit of massless neutrinos,  $\delta_i \rightarrow 0$ , we reproduce Källén's results.<sup>9</sup> The factors containing  $\bar{\delta}_i^2$  arise only from the phase-space integrations of the neutrinos, since the Fierz-rearranged form of the effective Lagrangian factorizes into a product of  $(\mu e)$  current and  $(\nu_i \nu_j)$  current.

The amplitude for the bremsstrahlung process [see Figs. 8(a) and 8(b)] is

$$\begin{aligned}
M = \frac{ieg^2}{8M_W^2} U_{ej} U_{\mu i}^\dagger \left[ \bar{u}(p_e) \gamma^\mu (1-\gamma_5) \frac{\not{p}_\mu - \not{k} + m_\mu}{(p_\mu - k)^2 - m_\mu^2} \not{\epsilon} u(p_\mu) \bar{u}(p_i) \gamma_\mu (1-\gamma_5) v(p_j) \right. \\
\left. + \bar{u}(p_e) \not{\epsilon} \frac{\not{p}_e + \not{k} + m_e}{(p_e + k)^2 - m_e^2} \gamma^\mu (1-\gamma_5) u(p_\mu) \bar{u}(p_i) \gamma_\mu (1-\gamma_5) v(p_j) \right], \quad (\text{A15})
\end{aligned}$$

where  $\epsilon^\lambda$  is the polarization vector of the emitted photon. It is trivial to check that  $M$  is gauge invariant. The differential decay rate for the process (2) is given by

$$(2E_e)(2\omega) \frac{d^6 R}{d^3 p_e d^3 k} = \frac{1}{2m_\mu} \frac{1}{(2\pi)^8} \int \frac{d^3 p_i}{2E_i} \int \frac{d^3 p_j}{2E_j} \delta^4(p_\mu - p_e - p_i - p_j - k) \sum_{e, \text{vspins}} |M|^2. \quad (\text{A16})$$

Next we integrate over the neutrinos' phase space (and sum over the photon polarization); in the usual four-dimensional space-time this gives

$$\begin{aligned} dR = & \frac{d^3 p_e}{2E_e} \frac{d^3 k}{2\omega} \frac{64}{(2m_\mu)} \frac{G_F^2 e^2}{(2\pi)^8} \\ & \times \left[ \left[ -\frac{m_\mu^2}{(k \cdot p_\mu)^2} - \frac{m_e^2}{(k \cdot p_e)^2} + \frac{2(p_e \cdot p_\mu)}{(k \cdot p_e)(k \cdot p_\mu)} \right] [A(p_e \cdot Q)(\bar{p}_\mu \cdot Q) + BQ^2(p_e \cdot \bar{p}_\mu)] \right. \\ & + \frac{(k \cdot \bar{p}_\mu)}{(k \cdot p_\mu)^2} [A(p_e \cdot Q)(k \cdot Q) + BQ^2(p_e \cdot k)] + \frac{1}{(p_e \cdot k)} [A(\bar{p}_\mu \cdot Q)(k \cdot Q) + BQ^2(\bar{p}_\mu \cdot k)] \\ & + BQ^2 \left\{ \frac{1}{(p_\mu \cdot k)^2} [(p_e \cdot k)(\bar{p}_\mu \cdot p_\mu) - (\bar{p}_\mu \cdot k)(p_\mu \cdot p_e)] + \frac{1}{(p_e \cdot k)^2} [(p_e \cdot k)(\bar{p}_\mu \cdot p_e) - (\bar{p}_\mu \cdot k)m_e^2] \right\} \\ & + A \frac{(p_e \cdot Q)}{(k \cdot p_\mu)^2} [(Q \cdot k)(p_\mu \cdot \bar{p}_\mu) - (k \cdot \bar{p}_\mu)(Q \cdot p_\mu)] - A \frac{(\bar{p}_\mu \cdot Q)}{(k \cdot p_e)^2} [(Q \cdot k)m_e^2 - (k \cdot p_e)(Q \cdot p_e)] \\ & + \frac{BQ^2}{(k \cdot p_\mu)(k \cdot p_e)} [(p_e \cdot p_\mu)(k \cdot \bar{p}_\mu) + m_e^2(k \cdot \bar{p}_\mu) - (k \cdot p_e)(p_\mu \cdot \bar{p}_\mu + p_e \cdot \bar{p}_\mu)] \\ & \left. + \frac{A(Q \cdot \bar{p}_\mu)}{(k \cdot p_\mu)(k \cdot p_e)} [(p_\mu \cdot p_e)(k \cdot Q) - (k \cdot p_e)(p_\mu \cdot Q)] - \frac{A(p_e \cdot Q)}{(k \cdot p_\mu)(k \cdot p_e)} [(k \cdot Q)(p_e \cdot \bar{p}_\mu) - (k \cdot \bar{p}_\mu)(p_e \cdot Q)] \right], \quad (\text{A17}) \end{aligned}$$

where

$$A = \frac{(\pi)^{3/2}(Q^2 - m^2)^2(2Q^2 + 4m^2)}{3\Gamma(3/2)(2)^4(Q^2)^3}, \quad (\text{A18a})$$

$$B = \frac{(\pi)^{3/2}(Q^2 - m^2)^3}{3\Gamma(3/2)(2)^4(Q^2)^3} \quad (\text{A18b})$$

with

$$\bar{p}_\mu = p_\mu - m_\mu s_\mu \quad (\text{A18c})$$

and

$$Q = p_\mu - p_e - k. \quad (\text{A18d})$$

This is infrared divergent in the limit  $\omega \rightarrow 0$ . To obtain the electron spectrum an integration over the photon space has to be performed and this is a divergent operation. To regularize this divergence we generalize to  $n$  dimensions the photon phase space

$$\frac{1}{(2\pi)^3} \frac{d^3 k}{2\omega} \rightarrow \frac{1}{(2\pi)^{n-1}} \frac{d^{n-1} k}{2\omega} = \frac{\pi^{(n/2)-1}}{(2\pi)^{n-1} \Gamma\left[\frac{n}{2}-1\right]} \int_0^{\omega_{\max}} d\omega \omega^{n-3} \int_{-1}^1 dz (1-z^2)^{(n/2)-2}, \quad (\text{A19})$$

where the maximum photon energy is given by

$$\omega_{\max} = \frac{1-x+\delta_e^2-\delta_i^2}{2[1-x/2+z/2(x^2-4\delta_e^2)^{1/2}]} \quad (\text{A20})$$

with  $z \equiv \cos\theta$  and  $\theta$  is the angle the photon is emitted with respect to the  $\hat{z}$  axis.

Thus, for the bremsstrahlung graph we have performed all the Dirac algebra first in four dimensions since the momenta involved are physical four vectors; continuation in  $n$  dimensions is performed only at the end. Thus, we have the contribution due to the photon bremsstrahlung process,

$$\begin{aligned}
 \frac{dR}{dx} = & \frac{e^2 G_F^2 m_\mu^5 x}{2(192\pi^5)} |U_{\mu u}|^2 |U_{ej}|^2 \left\{ \left[ \frac{-1}{n-4} + \ln 2\sqrt{\pi} - \frac{\gamma_E}{2} \right] [x(1-x)(1-\bar{\delta}_i^2)^3 \right. \\
 & \left. + x(2-x)(1-\bar{\delta}_i^2)^2(1+2\bar{\delta}_i^2)] \left[ 2 - \ln \left[ \frac{x^2}{\delta_e^2} \right] \right] \right. \\
 & + \{ x(1-x)[(1-\bar{\delta}_i^2)(1+\bar{\delta}_i^4) - (1-\bar{\delta}_i^2)^3 \ln(1-\bar{\delta}_i^2) - \bar{\delta}_i^4(-3+\bar{\delta}_i^2) \ln \bar{\delta}_i^2] \\
 & - x(2-x)[\bar{\delta}_i^2(1-\bar{\delta}_i^2)(-2+3\bar{\delta}_i^2) + \bar{\delta}_i^4(3-2\bar{\delta}_i^2) \ln \bar{\delta}_i^2 + (1-\bar{\delta}_i^2)^2(1+2\bar{\delta}_i^2) \ln(1-\bar{\delta}_i^2)] \\
 & - 2(1-x)^2(1-\bar{\delta}_i^2)^3 \} \left[ 2 - \ln \left[ \frac{x^2}{\delta_e^2} \right] \right] \\
 & - (1-x)^2 \left\{ \left[ 1 + \frac{(1-x/2)}{x} \ln \left[ \frac{x^2}{\delta_e^2} \right] \right] [3\bar{\delta}_i^4 \ln \bar{\delta}_i^2 + (1-\bar{\delta}_i^2)(-\frac{1}{2} + \frac{5}{2}\bar{\delta}_i^2 + \bar{\delta}_i^4)] \right. \\
 & \left. + \left[ 1 + \frac{(1-x)}{2x} \ln \left[ \frac{x^2}{\delta_e^2} \right] \right] [-\bar{\delta}_i^4(3+\bar{\delta}_i^2) \ln \bar{\delta}_i^2 + (1-\bar{\delta}_i^2)(\frac{1}{6} - \frac{4}{3}\bar{\delta}_i^2 - \frac{17}{6}\bar{\delta}_i^4)] \right\} \\
 & + [x(1-x)(1-\bar{\delta}_i^2)^3 + x(2-x)(1-\bar{\delta}_i^2)^2(1+2\bar{\delta}_i^2)] \\
 & \times \left[ - \left[ 1 + \frac{1}{x} \right] \ln(1-x) + \left[ \ln(1-x) + \frac{1}{2} \right] \ln \left[ \frac{x^2}{\delta_e^2} \right] + \text{Li}_2(x) - \frac{\pi^2}{6} - \frac{1}{4} \ln^2 \left[ \frac{\delta_e^2}{x^2} \right] \right] \\
 & - (\vec{\sigma}_\mu \cdot \hat{p}_e) x \left\{ \left[ \frac{1}{n-4} - \ln 2\sqrt{\pi} + \frac{\gamma_E}{2} \right] (1-\bar{\delta}_i^2)^2 [(1-x)(1-\bar{\delta}_i^2) - x(1+2\bar{\delta}_i^2)] \left[ 2 - 2 \ln \left[ \frac{x}{\delta_e} \right] \right] \right. \\
 & + [(1-x)(1-\bar{\delta}_i^2) - x(1+2\bar{\delta}_i^2)] (1-\bar{\delta}_i^2)^2 \left[ \left[ 1 + \frac{1}{x} \right] \ln(1-x) - 2 \ln(1-x) \ln(x/\delta_e) \right. \\
 & \left. + 2 \ln(1-\bar{\delta}_i^2)(1-\ln x/\delta_e) - \text{Li}_2(x) \right. \\
 & \left. \left. - \ln \left[ \frac{x}{\delta_e} \right] \frac{\pi^2}{6} + (\ln \delta_e - \ln x)^2 \right] \right. \\
 & + (1-x)(1-\bar{\delta}_i^2)^3 \left[ -2 + 3 \ln \frac{x}{\delta_e} \right] \\
 & + \{ (1-x)[-(1-\bar{\delta}_i^2)(1+\bar{\delta}_i^4) + \bar{\delta}_i^4(-3+\bar{\delta}_i^2) \ln \bar{\delta}_i^2] \\
 & - x[\bar{\delta}_i^2(1-\bar{\delta}_i^2)(-2+3\bar{\delta}_i^2) + \bar{\delta}_i^4(3-2\bar{\delta}_i^2) \ln \bar{\delta}_i^2] \} \left[ 2 - \ln \left[ \frac{x^2}{\delta_e^2} \right] \right] \\
 & + \frac{(1-x)^2}{x^2} [-3\bar{\delta}_i^4 \ln \bar{\delta}_i^2 + \frac{1}{2}(1-\bar{\delta}_i^2)(1-5\bar{\delta}_i^2-2\bar{\delta}_i^4)] \\
 & \times \left[ 2(1-x) + x \ln \frac{x}{\delta_e} + \frac{2(1-x)}{x} \ln(1-x) \right]
 \end{aligned}$$

$$\begin{aligned}
& + \frac{(1-x)^3}{x^2} \left[ -\bar{\delta}_i^4 (3 + \bar{\delta}_i^2) \ln \bar{\delta}_i^2 + (1 - \bar{\delta}_i^2) \left( \frac{1}{6} - \frac{4}{3} \bar{\delta}_i^2 - \frac{17}{6} \bar{\delta}_i^4 \right) \right. \\
& \times \left. \left[ -1 + \frac{(x-2)}{(1-x)} + \ln \frac{x}{\delta_e} - \frac{2}{x} \ln(1-x) \right] + \frac{(1-x)}{x} (1 - \bar{\delta}_i^2)^3 \left[ x \ln \frac{x}{\delta_e} - 2x \right] \right] \Bigg] . \quad (A21)
\end{aligned}$$

The infrared divergence appears as a pole in  $n - 4$ . This precisely cancels that in the virtual corrections [see (A12)] and we obtain the final expression given in Eqs. (10c) and (10d). As noted in Ref. 14, to obtain the result of the cutoff method all we need is to substitute

$$\frac{1}{4-n} - \frac{1}{2} \gamma_E + \ln 2 \sqrt{\pi} \rightarrow \ln \lambda_{\min} , \quad (A22)$$

where  $\lambda_{\min}$  is the cutoff photon energy. If the photon energy spectrum is measured in addition to and distinguished from the electron energy, then this cutoff is replaced by the energy resolution of the apparatus.

- 
- <sup>1</sup>L. Michel, Proc. Phys. Soc. London **A63**, 514 (1950).  
For a concise, updated review of classical theory of weak interactions, see A. Sirlin, in *Proceedings of the TRIUMF Muon Physics Workshop, Vancouver, 1980*, edited by J. A. MacDonald, J. N. Ng, and A. Strathdee (TRIUMF, Vancouver, 1981), p. 81.
- <sup>2</sup>S. Weinberg, Phys. Rev. Lett. **19**, 1264 (1967); A. Salam, in *Elementary Particle Theory: Relativistic Groups and Analyticity (Nobel Symposium No. 8)*, edited by N. Svartholm (Almqvist and Wiksell, Stockholm, 1968).
- <sup>3</sup>D. A. Ross, Nucl. Phys. **B51**, 116 (1973).
- <sup>4</sup>The effective  $\rho$  parameter is obtained by integrating the  $e^+$  spectrum out to the value of  $x = 0.95$  where  $x \equiv 2E_e/m_\mu$ . This effective value will change when a larger value of  $x$  is included. See A. Sirlin, in *Muon Physics II*, edited by V. W. Hughes and C. S. Wu (Academic, New York, 1975), p. 49.
- <sup>5</sup>A. Sirlin and T. Kinoshita, Phys. Rev. **113**, 1652 (1959).
- <sup>6</sup>J. Eggers, in *Proceedings of the VIII International Conference on High Energy Physics and Nuclear Structure*, edited by D. Measday and A. W. Thomas (North-Holland, Amsterdam, 1979), p. 87.
- <sup>7</sup>J. N. Ng, Phys. Lett. **99B**, 53 (1981); Nucl. Phys. **191B**, 125 (1981).
- <sup>8</sup>P. Kalyniak and J. N. Ng, Phys. Rev. D **24**, 1874 (1981). See also R. Shrock, Phys. Rev. D **24**, 1275 (1981).
- <sup>9</sup>An excellent treatment of the radiative corrections in the  $V-A$  theory with massless neutrinos is given by G. Källén, in *Springer Tracts in Modern Physics* (Springer, Berlin, 1970) Vol. 46, p. 67.
- <sup>10</sup>Experimental supports are given by the measurement of  $\beta$  decay of tritium [see V. A. Lyubimov *et al.*, Phys. Lett. **94B**, 266 (1980)] and the  $\pi \rightarrow \mu \nu$  decay spectrum [see M. Daum *et al.*, Phys. Rev. D **20**, 2692 (1979); R. Abela *et al.*, Phys. Lett. **105B**, 263 (1981)].
- <sup>11</sup>If intermediate-mass Majorana neutrinos exist they can give rise to  $CP$ -violating effects. The size of such effects will be controlled by  $(m_\nu/m_\mu)^2$  and the magnitude of the mixing angles between the IMN's and the light neutrinos, as well as the  $CP$ -violating phase. For a lucid discussion see R. H. Pratt, Phys. Rev. **111**, 649 (1958).
- <sup>12</sup>Determination of the  $\tau$ -neutrino mass is given by J. Kirby, in *Proceedings of the 1979 International Symposium on Lepton and Photon Interactions at High Energies, Fermilab*, edited by T. B. W. Kirk and H. D. I. Abarbanel (Fermilab, Batavia, Illinois, 1980), p. 107. The value is  $m_{\nu_\tau} < 250 \text{ MeV}/c^2$ .
- <sup>13</sup>G. 't Hooft and M. Veltman, Nucl. Phys. **B44**, 189 (1972).
- <sup>14</sup>W. Marciano and A. Sirlin, Nucl. Phys. **B88**, 86 (1975). See also R. Gastmaus and R. Meuldermaus, *ibid.* **B63**, 277 (1973).
- <sup>15</sup>For the three-neutrinos case with HNN mixing the factors before  $R_0$  and  $R_3$  reduce to  $|U_{\tau 3}|^2$  and  $|U_{\mu 3}|^2$ , respectively.
- <sup>16</sup>T. D. Lee and M. Nauenberg, Phys. Rev. **133**, 1549 (1964); T. Kinoshita, J. Math. Phys. **3**, 650 (1962).
- <sup>17</sup>We have also checked that the correction to the muon lifetime due to massive neutrinos does not contain  $\ln \delta_e$  terms in accordance with the Lee-Nauenberg-Kinoshita theorem.

<sup>18</sup>This information can also be obtained from a measurement of the branching ratio  $\pi \rightarrow e\nu/\pi \rightarrow \mu\nu$ . See R. Shrock, Phys. Lett. **96B**, 159 (1980); see also Ref. 7.

<sup>19</sup>M. Bardon *et al.*, Phys. Rev. Lett. **14**, 449 (1965).

More recent measurement is now underway in an

LBL-TRIUMF experiment, E-176; K. Crowe, private communication.

<sup>20</sup>We use the metric convention of J. D. Bjorken and S. Drell, *Relativistic Quantum Fields* (McGraw-Hill, New York, 1965).